AD-A108 128 MISSOURI UNIV-ROLLA DEPT OF PHYSICS F/G 20/5
KINETIC PROCESSES IN HIGH PRESSURE GASES: EXCITED STATE COLLISI--ETC(U)
DEC 81 L D SCHEARER, R H MCFARLAND N00014-75-C-0477
UNCLASSIFIED TR-14 NL

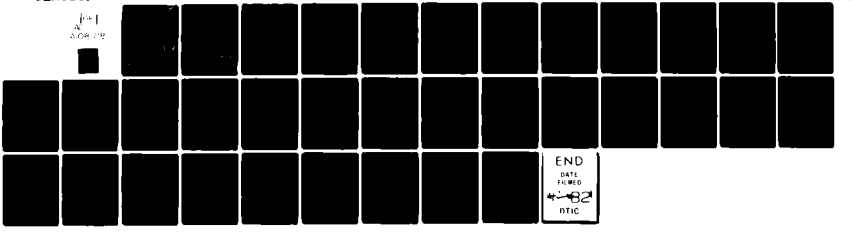

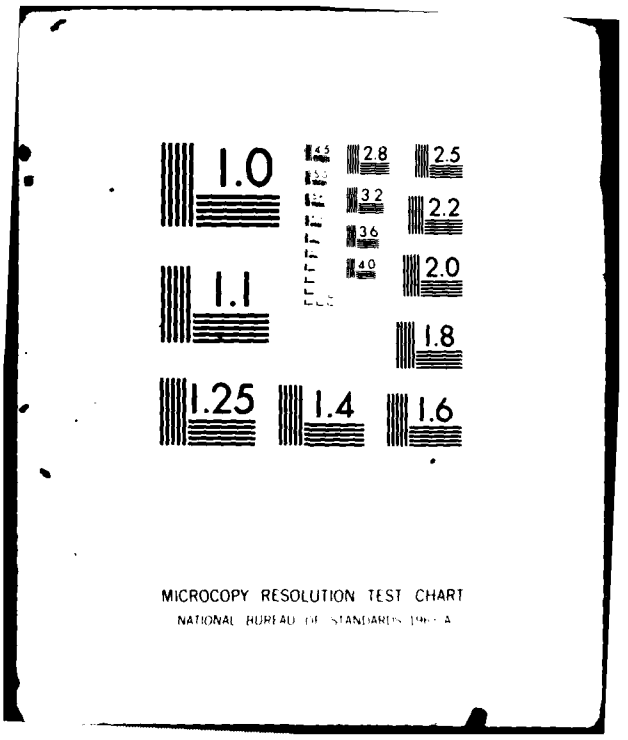
1.0
1.1
1.25
1.4
1.6
1.8
2.0
2.2
2.5
2.8
3.2
3.6
4.0
MICROCOPY RESOLUTION TEST CHART
NATIONAL BUREAU OF STANDARDS 1963-A

Unclassified

SECURITY CLASSIFICATION OF THIS PAGE (When Data Entered)

LEVEL II AD A092663 12

REPORT DOCUMENTATION PAGE		READ INSTRUCTIONS BEFORE COMPLETING FORM
1. REPORT NUMBER 14	2. GOVT ACCESSION NO. AD-A108128	3. RECIPIENT'S CATALOG NUMBER
4. TITLE (and Subtitle) Kinetic Processes in High Pressure Gases: Excited State Collisions		5. TYPE OF REPORT & PERIOD COVERED Technical Report Dec. 80-Dec. 81 6. PERFORMING ORG. REPORT NUMBER
7. AUTHOR(s) L. D. Schearer		8. CONTRACT OR GRANT NUMBER(s) ONR N00014-75C-0477
9. PERFORMING ORGANIZATION NAME AND ADDRESS The Curators of the University of Missouri for the University of Missouri-Rolla, Rolla, MO 65401		10. PROGRAM ELEMENT, PROJECT, TASK AREA & WORK UNIT NUMBERS NR 343 011
11. CONTROLLING OFFICE NAME AND ADDRESS Department of the Navy Office of Naval Research Washington, D.C. 20360		12. REPORT DATE 1 Dec. 1981 13. NUMBER OF PAGES
14. MONITORING AGENCY NAME & ADDRESS(if different from Controlling Office)		15. SECURITY CLASS. (of this report) Unclassified 15a. DECLASSIFICATION/DOWNGRADING SCHEDULE

16. DISTRIBUTION STATEMENT (of this Report)

Approved for public release: Distribution unlimited.

17. DISTRIBUTION STATEMENT (of the abstract entered in Block 20, if different from Report)

DTIC ELECTE S DEC 7 1981 D

18. SUPPLEMENTARY NOTES

19. KEY WORDS (Continue on reverse side if necessary and identify by block number)

line shifts, line broadening, recombination, associative excitation, Rydberg atoms, electron density measurements, Saha equilibrium, sodium vapor

20. ABSTRACT (Continue on reverse side if necessary and identify by block number)

A dense sodium vapor in a high pressure buffer of argon has been simultaneously excited by shoft (4 ns) laser pulses from two lasers: the first tuned to one of the D line transitions at 589 nm and the second tuned to the photoionization threshold of the 3p states near 406 nm. The temporal evolution of the system was studied with and without the photoionizing laser pulses. At early times (~ 100 ns) excited state populations are determined by energy transfer collisions between two laser-excited 3p atoms while the ion/electron

DD FORM 1 JAN 73 1473 EDITION OF 1 NOV 65 IS OBSOLETE
S/N 0102-LF-014-6601

SECURITY CLASSIFICATION OF THIS PAGE (When Data Entered)

density is controlled by superelastic heating of "seed" electrons followed by electron impact ionization of excited state atoms. At late times (~ 1 μs) excited state populations are controlled by collisional-radiative recombination processes. Excitation transfer rates into the 4d, 5d, 6d, and 6s levels are measured. The optical emission spectra of a recombining Na plasma is observed. The shift and broadening of the spectral line emission due to electron collisions is observed and the electron density calculated from shift measurements. The results agree well with electron densities obtained in the same system from Saha plots of excited state densities.

TECHNICAL REPORT

KINETIC PROCESSES IN HIGH PRESSURE GASES: EXCITED STATE COLLISIONS

L. D. Schearer

Department of Physics

University of Missouri-Rolla

Rolla, MO 65401

Technical Report to the Office of Naval Research.
Grant No. N00014-75-C-0477 for the period December 1980 - December 1981.

CONTENTS

PERSONNEL ON CONTRACT

Principal Investigator

Prof. Laird D. Schearer
Prof. Robert H. McFarland

Associates

Mr. Danny Krebs, Graduate Assistant
Mr. Johnny Daniels, Graduate Assistant
Mr. Mark Fraser, Graduate Assistant

CONTRACT DESCRIPTION

The purpose of the research program is to investigate energy exchange and energy loss mechanisms in discharge plasmas and their afterglows. Specific mechanisms which have been investigated in our laboratory include: (a) metastable interactions, such as dissociative excitation and Penning ionization, (b) collisional broadening and level shifts in excited states produced by the presence of a buffer gas and/or electrons, and (c) electron loss mechanisms due to volume recombination.

I. INTRODUCTION

This research program deals with the kinetic and radiative processes occurring in a dense mixture of alkali vapor and a noble gas buffer which has been excited by short, powerful laser pulses.

A variety of devices, including atmospheric pressure lasers, high current/low inductance switches, high efficiency lamps, and inertial confinement fusion targets utilize similar, excited atomic vapors at high pressures. With the current interest in these devices, the role of collisional and radiative processes involving highly excited (Rydberg) states has taken on a new importance. A common feature of all these devices is that energy is deposited into the system in the form of large densities of ion/electrons, metastable species, and various excited neutrals. This energy is then transferred to some desired channel; e.g., a lasing transition, electron production, electron heating, etc. The efficiency of this energy transfer and, indeed, the efficiency of the initial excitation process, depend on the specific collisional and radiative processes occurring in the mixture. For instance, radiation loss depends strongly on the degree of radiation trapping, which in turn, depends on the collisional linewidths and shifts of the transitions involved.

The general experimental approach of this work consists of exciting the mixture in a time short compared to the time in which the system relaxes. The behavior of a freely relaxing system may then be related to the fundamental processes occurring in the system. This is the rationale behind our earlier conventional afterglow experiments which have yielded a great deal of information regarding the behavior of gaseous discharges at lower pressures[1].

The present work differs from conventional afterglow experiments in that the latter use some form of microwave or radio frequency breakdown as the source of excitation, whereas this work uses optical frequency (laser) excitation. The absorption of optical energy from high power laser pulses may be well characterized, and therefore the initial conditions of the excited vapor are well known. In contrast, microwave and radio frequency breakdown are typically stochastic and the initial conditions of the excited system varies substantially from pulse to pulse. Furthermore, microwave and radio frequency breakdown is difficult to achieve at the high pressures with which this study is concerned.

II. PROGRESS REPORT

Kinetic processes in Na + R.G. mixtures have been examined for rare gas densities between 400 and 2000 Torr and Na densities up to 1 Torr. Electron/ion densities up to 10^{15} cm^{-3} are obtained under typical experimental conditions.

We have measured associative excitation rates for Na(3p) + Na(3p) → Na(4,5,6d n 6s) + Na(3s) collisions, spectral line shifts due to buffer gas collisions and stark shifts due to electron collisions, and electron densities and electron temperatures in the afterglow of high power laser pulses.

A. EXCITATION TRANSFER COLLISIONS AND ELECTRON SEEDING PROCESSES IN A RESONANTLY EXCITED SODIUM VAPOR

A number of interesting effects occur when a dense sodium vapor is excited by laser radiation tuned to one of the D lines. In particular, (1) complete ionization has been observed when high power, pulse lasers are employed[2] and (2) surprisingly high densities of atoms are observed in the nd (n=3,4,5) and ns (n=5,6) levels when a CW laser is employed[3].

Theoretical calculations[4] indicate that the ionization present in the first case is due to electron heating via superelastic collisions followed by electron impact ionization. A small initial number of electrons (seed electrons) is supplied by several, comparatively weak mechanisms including associative ionization and two photon ionization of the 3p state atoms.

The mechanisms responsible for the observations in the second case are, perhaps, less well understood. Allegrini, et al. attributed the excited atom densities to collisions involving two 3p atoms[3]:

$$Na\ (3p) + Na\ (3p) \rightarrow Na\ (3s) + Na\ (n\ell) \pm K.E.$$

While such an excitation transfer mechanism explains an apparent dependence of the Na ($n\ell$) density on the square of the 3p density, there was some doubt whether the cross-section for this process is large enough to account for the Na ($n\ell$) densities observed. Bearman and Levanthal[5], in an experiment similar to that of Allegrini, et al. did not observe excitation of levels lying more than $\sim$ 3 KT above the energy of two Na (3p) atoms.

The interplay of excitation transfer collisions and electron seeding processes is possible with both CW excitation and excitation with pulsed lasers. In the experiment described here we were able to separate the excitation transfer effects from the effects of the electron impact excitation and ionization by observing the time dependent fluorescence decay from various excited states under two sets of initial conditions: (1) one in which the seed electron density was less than 10^7 cm^{-3} and (2) one in which the seed electron density was $\gtrsim 10^{12}$ cm^{-3}. In both cases the initial density of 3p atoms was about 10^{15} cm^{-3}. From differences in the behavior of the excited state populations under these two conditions we were able to distinguish between processes involving electron collisions and those which do not. In order to observe these effects on a time resolved basis, we used short (4 ns) laser pulses to excite the 3p states and create the initial electron density. The experimental arrangement is shown in Fig. 1. Kopystynska and Kowalczyk[6] had earlier used short laser pulses to excite the D lines and observe subsequent radiative emission from excited nd and ns states; however, they made no attempt to independently vary the seed electron concentration by using a second ionizing laser pulse as is described in this experiment.

Figure 2 shows the fluorescence of the 5d → 3p transition versus time when both lasers are employed. The optical emission from the cell consists of two components: a strong initial fluorescence pulse of approximately 100 ns duration followed by the rise and slow decay of fluorescence due to excited states created in the 3-body, electron stabilized recombination process which extended beyond 20 μsec. Figure 3 is a wavelength scan of the recombination fluorescence 2 μs after the lasers have fired. The detecting apparatus was calibrated against the emission of a standard quartz-iodine lamp to permit absolute measurements of the excited state densities. A Saha-Boltzmann plot of the absolute excited state densities for levels above the 7d state yields an electron density of 1×10^{14} cm^{-3} at 2 μsec after the lasers are fired. Stark shifts of the $6^2D \rightarrow 3^2P$ and $7^2D - 3^2P$ due to the electrons were also measured. It was necessary in a separate experiment to determine the shift due to the argon buffer gas[7] and subtract the two shifts to obtain the shift due to electron collisions. The results agreed well with Griem's predictions for $N_e \cong 10^{14}$ cm^{-3}.[8] For reasons detailed below, the electron density immediately after the lasers have fired is considerably smaller than it is 2 μsec later.

With the ionizing (406 nm) laser off, the recombination fluorescence disappeared, indicating an absence of strong ionization. The early fluorescence pulse generally remained albeit altered in magnitude and shape. Less than one percent of the ionizing laser pulse at 406 nm is absorbed.

Figure 4 shows the level of the 3p → 3s resonance fluorescence with and without the ionizing laser pulse. It may be seen in Fig. 4, and is apparent in traces from the fast oscilloscope, that the 3p population is not significantly changed by the ionizing laser in the first 30 ns after

the lasers have fired. At later times, however, the 3p population is depleted about 16% by the presence of the ionizing laser pulses, which are virtually synchronous with the resonant laser pulses. Thus, we believe that the ionization is enhanced by the electron seeding process suggested by Measures, with direct photoionization by the ionizing laser providing the seed electrons. In this model, the energy of any free (seed) electrons is rapidly increased by superelastic collisions with the large density of excited 3p atoms. Subsequently, ionization proceeds via electron impact excitation and ionization of the excited atoms. The number of seed electrons provided by the ionizing laser is $\sim 10^{12}$ cm^{-3} since the photoionization cross section is large near threshold.

The 589 nm and 406 nm lasers can excite high vibrational levels of the $A\ ^1\Sigma$ and $B\ ^1\pi$ states of the dimer, respectively. Some weak dimer emission was seen in the early fluorescence. The recombination fluorescence and early atomic fluorescence disappeared when the resonant laser was detuned by a few angstroms, indicating a dependence of these signals on the presence of large concentrations of Na (3p) atoms. Thus dimer absorption does not play a role in the excitation and ionization processes in this experiment.

Figure 4 shows the strong initial fluorescence pulse for several transitions both with and without the ionizing laser. Without the ionizing laser, the rise of the fluorescence pulse is rapid for the 4d → 3p fluorescence and considerably slower for the 5d → 3p and 6d → 3p transitions. With the ionizing laser on, the 4d population declines by about 25%. The 5d and 6d populations exhibit a more rapid rise and decay, than they do with the ionizing laser off. We measured the

population densities corresponding to each level based on the calibration of our detection system as previously mentioned.

With the ionizing laser on, the electron density is several orders of magnitude greater than when it is off. The electron temperature is not altered greatly, however, because the electron temperature is controlled by the 3p population[4] which is not greatly changed. If the production of atoms in the ns and nd states were due to electron impact excitation, the fluorescence from these levels would increase dramatically when the ionizing laser is on. This does not occur and therefore electron collisions are not the source of the nd and ns populations in this experiment.

Traces from the fast oscilloscope indicate that the rise of the 4d population occurs about 10 ns after the laser pulse has passed and does not peak until about 30 ns after the 3p population has peaked. Since the laser pulses are only 4 ns in duration (FWHM), any radiative absorption process involving the laser pulses cannot be responsible for the 4d population. We considered and excluded the possibility that trapped resonance radiation might be absorbed in the far wings of the $3p \rightarrow 4d$ and $3p \rightarrow 5s$ transitions. Since the photon energy density of the trapped radiation is several orders of magnitude smaller than that of the laser, this explanation does not fit the observed time dependence.

The excitation transfer process originally proposed by Allegrini et al.[3],

$$Na(3p) + Na(3p) \rightarrow Na(n\ell) + Na(3s) + K.E. \qquad (1)$$

appears to be the primary source of the 4d, 5d, 6d and 6s population in the

early afterglow. We thus write,

$$N_{3p}(t) = N_{3p}(0) \exp(-t/\tau^*_{3p}) \tag{2}$$

where τ^*_{3p} is the trapped lifetime of the 3p state, and

$$\frac{dN_{n\ell}(t)}{dt} = -\frac{N_{n\ell}}{\tau_{n\ell}} + k_{n\ell}[N_{3p}(5)]^2 \tag{3}$$

where $\tau_{n\ell}$ is the effective lifetime of the $n\ell$ state and $k_{n\ell}$ is the rate constant for the production of the $N_{n\ell}$ atoms by the excitation transfer process of (1). Equation (3) is easily solved to yield

$$N_{n\ell}(t) = k_{n\ell}[N_{3p}(0)]^2 \tau^*_{3p} \tau_{n\ell}[\tau^*_{3p} - 2\tau_{n\ell}]^{-1}$$
$$X [\exp(-2t/\tau^*_{3p}) - \exp(-t/\tau_{n\ell})] \tag{4}$$

Kopystynska and Kowalczyk[6] showed that equation (4) fits the time dependence of their experimental data quite well. We also found that equation (4) fits our data as shown in Fig. 5 although the effective decay rates are shorter than the natural radiative lifetimes. This is not surprising considering the bi-exponential form of the decay from these excited levels at our high buffer pressures[9].

If this interpretation is correct, we can obtain estimates of $K_{n\ell}$ by fitting equation (4) to the experimental curves. A fit to the 4d - 3p observations is shown in Fig. 5. From this we obtain $K_{4d} = 1 \times 10^{-12}$ cm^{-3} sec^{-1} and $\tau_{4d} = 39$ nsec. Extending this analysis to the other states, we obtain the data in Table (1). The absolute uncertainty of the $K_{n\ell}$ measurements is about an order of magnitude, due principally to uncertainty in the 3p population. The relative accuracy of these data should be

quite good since there is little uncertainty in the relative populations in the nd and ns states.

Kowalczyk[11] has modeled the excitation transfer collision of two Na (3p) atoms using adiabatic molecular potentials. In this model, the cross-section for excitation transfer depends strongly on the electric dipole matrix elements connecting the Na (3p) level to the highly excited Na ($n\ell$) level. Since for excitation to a Na (np) level, this matrix element is zero, corresponding to a dipole-forbidden transition, we expect that the rate constants for 4p and 5p formation measured by Kushawaha and Levanthal[10] to be significantly smaller than the 4d, 5d, 6d, and 6s rate constants reported here. The calculated cross section for excitation transfer to the 4d state is 6.1×10^{-16} cm^2 at T = 650°K[11]. This corresponds to a rate constant of 5×10^{-11} cm^3 sec^{-1} which is to be compared with the value of 1×10^{-12} cm^3 sec^{-1} obtained in this experiment. The results are summarized in Table 1.

We note that the rate constants reported in Table 1 decrease dramatically as the energy defect increases from 1.2 KT to 8.7 KT. The reduction in the rate constant follows approximately the reduction in the fraction of atoms in a Boltzmann distribution which have kinetic energies greater than the energy defect. This behavior is consistent with the theoretical model of Kowalczyk.

We note that the nd levels are strongly coupled to higher angular momentum levels by mixing collisions with the buffer gas[9]. As a result, the degeneracy of these levels is effectively $2N^2 - 8$. The net population in all these excited levels represents a significant pool of target atoms for electron impact ionization. Perhaps the electron seeding

models should incorporate excitation transfer mechanisms as more rate constant data becomes available.

B. ELECTRON DENSITY MEASUREMENTS IN A LASER INDUCED Na PLASMA

A variety of techniques exist for the determination of the electron density in a decaying plasma; however, spectral measurements have the advantage that non-contact observations can be made and small volumes sampled within small time intervals.

We have observed spectral line shifts and broadening due to electron collisions in a recombining Na plasma. From measurements of the spectral line shifts, the electron density is calculated. The electron density thus obtained is compared with measurements inferred from Saha-Boltzmann plots of the excited Na states in local thermodynamic equilibrium with the electrons. These electron density measurements are also compared with charge removed from the plasma by an applied electric field. The plasma for the experiment described here consists of a line charge of approximately 0.5 mm diameter with electron densities up to 10^{15} cm^{-3} in a cell containing Na ($\sim$ 1 Torr) and Argon (400 Torr).

The sodium atoms are ionized in a 2 photon, resonant absorption process via the 3p state. The laser intensities and pulse widths (50 μjoules, 4 nsec) do not produce more than a relatively small number ($\sim 10^{12}$ cm^{-3}) of "seed" electrons via the photoionization process. However, collisional mechanisms involving densely populated excited states and the seed electrons can lead to nearly complete ionization of the Na vapor.

The fluorescence appearing 2 μs after the laser pulses is due to the recombination process. With the Boxcar Integrator set to a delay

TABLE I. Values of $k_{n\ell}$ and magnitudes of the energy defects.

Level	$k_{n\ell}$ ($cm^3\ s^{-1}$)	$(E_{n\ell} - 2E_{3p})/KT$
$4d^{(a)}$	1×10^{-12}	1.2
$4d^{(b)}$	5×10^{-11}	1.2
$5d^{(a)}$	5.2×10^{-14}	6.1
$6d^{(a)}$	8.6×10^{-15}	8.7
$6s^{(a)}$	7.6×10^{-15}	4.8
$4p^{(c)}$	6.1×10^{-16}	-10.8
$5p^{(d)}$	7×10^{-18}	3.1

(a) This work, T = 397°C.

(b) Calculated from Ref. 11, T = 377°C.

(c) Taken from Ref. 10, T = 214°C.

(d) Taken from Ref. 10, T = 243°C.

of 2 μs and 0.5 μs aperture a monochromator scan of the emission produces the spectrum shown in Fig. 3. The monochromator detection system is calibrated against an absolute standard lamp; thus absolute intensity measurements of the transitions along with radiative decay rates yield absolute excited state densities.

The recombination spectrum shown in Fig. 3 is obtained by scanning the monochromator through the respective transitions with the synchronous photon counter set for a delay of 2 μsec after the laser pulses and with an aperture of 1.0 μsec. The emission lines are thus shifted (and broadened) both by collisions with electrons and the 400 Torr argon buffer. Figure 6 is a high-resolution monochromator scan of the 6d-3p transition under these conditions.

In Fig. 7 the line shifts for the 3p-5d, 6d, and 7d transitions are shown. The upper curve indicates line shifts associated with both buffer gas and electron collisions. The lower curve reflects shifts due to the buffer gas alone (next section). The difference in the shifts between the two curves is then due to the difference in the electron density under the two conditions. The results are summarized in Table II.

Line shifts in Na due to collisions with electrons have been computed theoretically by Griem[8]. In Fig. 8 the results obtained by Griem are extrapolated to 900°K and an electron density of 6.8×10^{14} cm^{-3} and shown as circles. A solid line connects the computed shifts to aid the eye. The square points are the experimental shifts we measure by the technique outlined in the preceding sections. A dotted line connects the experimental points. The 900°K electron temperature was derived from our

Table II

Electron Density (cm^{-3})	Method
3.4×10^{14}	Saha-Boltzman Plot
4.1×10^{14}	Stark Shift (5d → 3p)
7.1×10^{14}	Stark Shift (6d → 3p)
7.0×10^{14}	Stark Shift (7d → 3p)
3.0×10^{14}	Charge Extraction

Saha plots. The 6.8×10^{14} cm^{-3} yields the best fit of the theoretical data of Griem to our experimental results.

C. PRESSURE SHIFTS: THREE PHOTON ABSORPTION PROCESSES

The optical emission from the ionized volume at times greater than 0.5 μs after the laser pulse can be described in terms of collisional-radiative recombination processes. If one integrates this emission signal over all times and over all wavelengths, the number of photons collected is proportional to the total number of ion-electrons formed in the excitation-ionization process.

If the second (blue) laser is tuned through a 3p-nd (ns) transition, the number of "seed" electrons produced is proportional to the transition moment, the laser intensity, and the photoionization cross section of the nd (ns) state. The "seed" electron density in turn determines the ultimate ion/electron density. If we observe the integrated emission from the interaction zone and scan the frequency of the second laser, we obtain the spectrum shown in Fig. 9. Since the excitation of the nd (ns) excited state takes place only during the 4 ns laser pulse, well before the ion/electron density reaches its peak, the shift of the spectral lines as observed while tuning the blue laser through a transition is *due only to the presence of the buffer gas*. A higher resolution tracing as the laser is scanned through the 3p-8d transition at 439 nm is shown in Fig. 10. The ion yield is recorded simultaneously in a cell with no buffer gas and a cell with 400 Torr of Argon buffer. Two components appear in the high pressure scan representing the $3P_{1/2}$ and $3P_{3/2}$ levels which are collisionally mixed at the high buffer gas pressures. The shift in the emission lines due to the Ar buffer at 400 Torr is then simply determined. The spectral line shifts for the 3p-nd transitions through n=18 are shown in Fig. 11.

REFERENCES

1. L. D. Schearer, Phys. Rev. 10, 1380 (1974).

2. (a) T. B. Lucatorto and T. J. McIlrath, Phys Rev Lttt, 37 428 (1976); (b) T. J. McIlrath and T. B. Lucatorto, ibid, 38 1390 (1977).

3. M. Allegrini, G. Alzetta, A. Kopystynska, L. Moi and G. Orriols, Opt. Common, 19, 96 (1976).

4. R. M. Measures and P. T. Cardinal, Phys. Rev. A, 23, 804 (1981).

5. G. H. Bearman and J. J. Leventhal, Phys. Rev. Lett., 41, 1227 (1978).

6. A. Kopystynska and P. Kowalczyk, Opt. Commun., 25, 351 (1978).

7. D. Krebs and L. D. Schearer, "33rd Annual Gaseous Electronics Conference", (Univ. of Oklahoma, Oct., 1980).

8. H. R. Griem, "Plasma Spectroscopy", (McGraw-Hill, New York, 1964).

9. T. F. Gallagher, S. A. Edelstein, and R. M. Hill, Phys. Rev. A, 15, 1945 (1977).

10. V. S. Kushawaha and J. J. Leventhal, Phys. Rev. A, 22, 2468 (1980).

11. P. Kowalczyk, Chem. Phys. Lett., 68, 203 (1975).

Figure 1. Schematic of the Apparatus.

Figure 2. Fluorescence intensity versus time after laser excitation for the 5d → 3p transition with both lasers employed. The early fluorescence peak, which is off-scale, is approximately 20 times more intense than the peak of the recombination fluorescence at t = 2 μs.

Figure 3. Recombination fluorescence at t = 2 μs versus wavelength. Scan resolution is .8 nm (FWHM).

Figure 4. Early fluorescence intensity for various transitions versus time. Resonance fluorescence for the 3p - 3s transition is not calibrated relative to that of the nd → 3p transitions. Otherwise the relative intensities are as indicated. Lighter traces were taken with both lasers employed. Dark traces were taken with only the laser tuned to 589 nm employed.

Figure 5. Fluorescence intensity of the 4d → 3p transition versus time. The solid curve is experimentally derived. The dashed curve was calculated using equation (4).

Figure 6. Simultaneous high resolution scan of plasma emission and lamp emission.

Figure 7. Shift versus principal quantum number for $3^2P_{3/2} \rightarrow n^2D$ transitions as determined from scans of the plasma emission (+) and absorption measurements (Δ) with .43 Amagats of argon buffer.

Figure 8. Stark Shift versus principal quantum number calculated by Griem for T_e = 10,000°K, $n_e = 6.8 \times 10^{14}$ cm^{-3} (+), T_e = 900°K, $n_e = 6.8 \times 10^{14}$ cm^{-3} ( ); and experimental points ( ).

Figure 9. Scan of ion yield versus the wavelength of the second, ionizing laser. The ionization limit corresponds to a wavelength of 408 nm.

Figure 10. Ion yield versus laser wavelength for the 3p → 8d transitions from a scan taken simultaneously in a cell with 400 torr of argon buffer and a cell with no buffer gas. Two components are present in the high pressure cell due to collisional mixing of the $3^2P_{3/2, 1/2}$ levels.

Figure 11. Spectral line shifts as a function of principal quantum number 3p - nd. Argon-Na at 400 Torr.

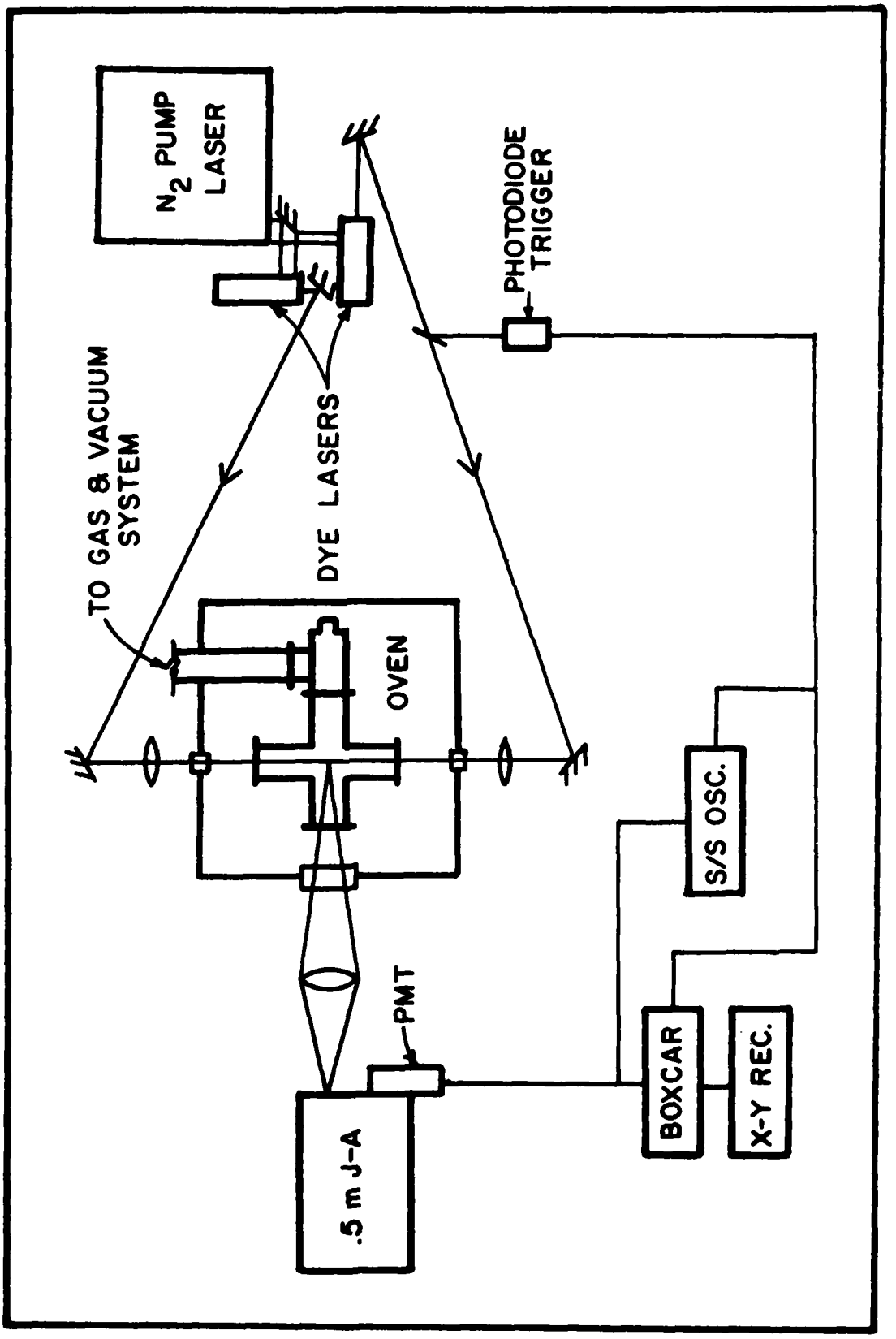
N_2 PUMP LASER
PHOTODIODE TRIGGER
TO GAS & VACUUM SYSTEM
DYE LASERS
OVEN
S/S OSC.
PMT
BOXCAR
X-Y REC.
.5 m J-A

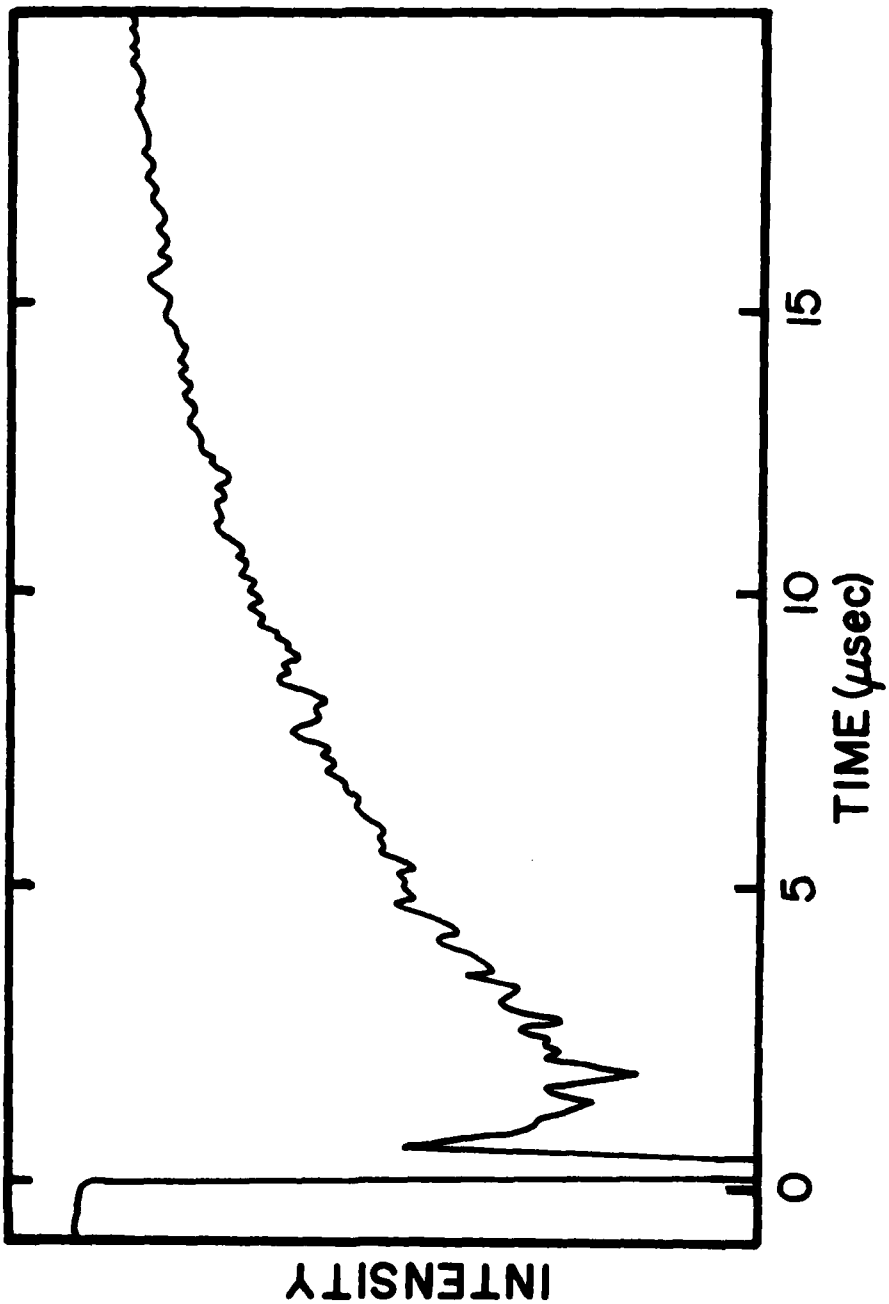
INTENSITY
0
5
10
15
TIME (μsec)

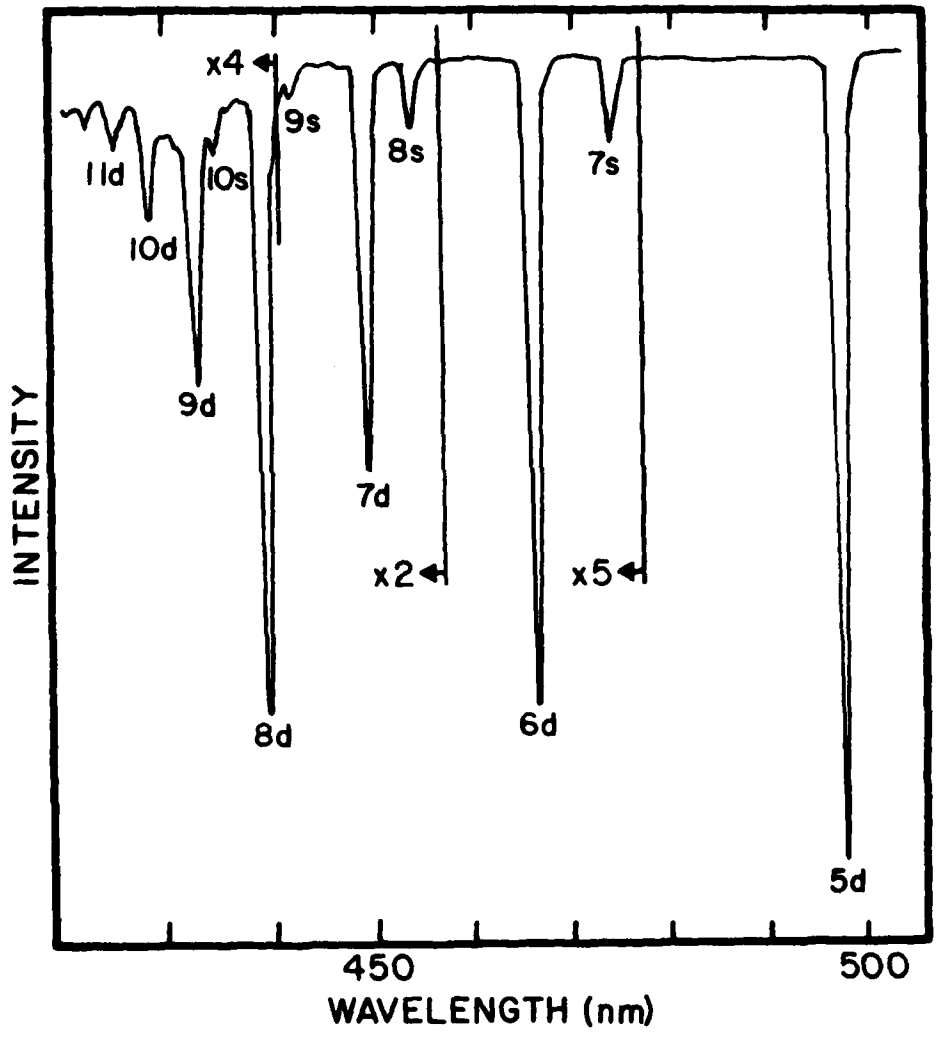
x4
11d
10d
9d
10s
9s
8d
8s
7d
x2
7s
x5
6d
5d
INTENSITY
450
500
WAVELENGTH (nm)

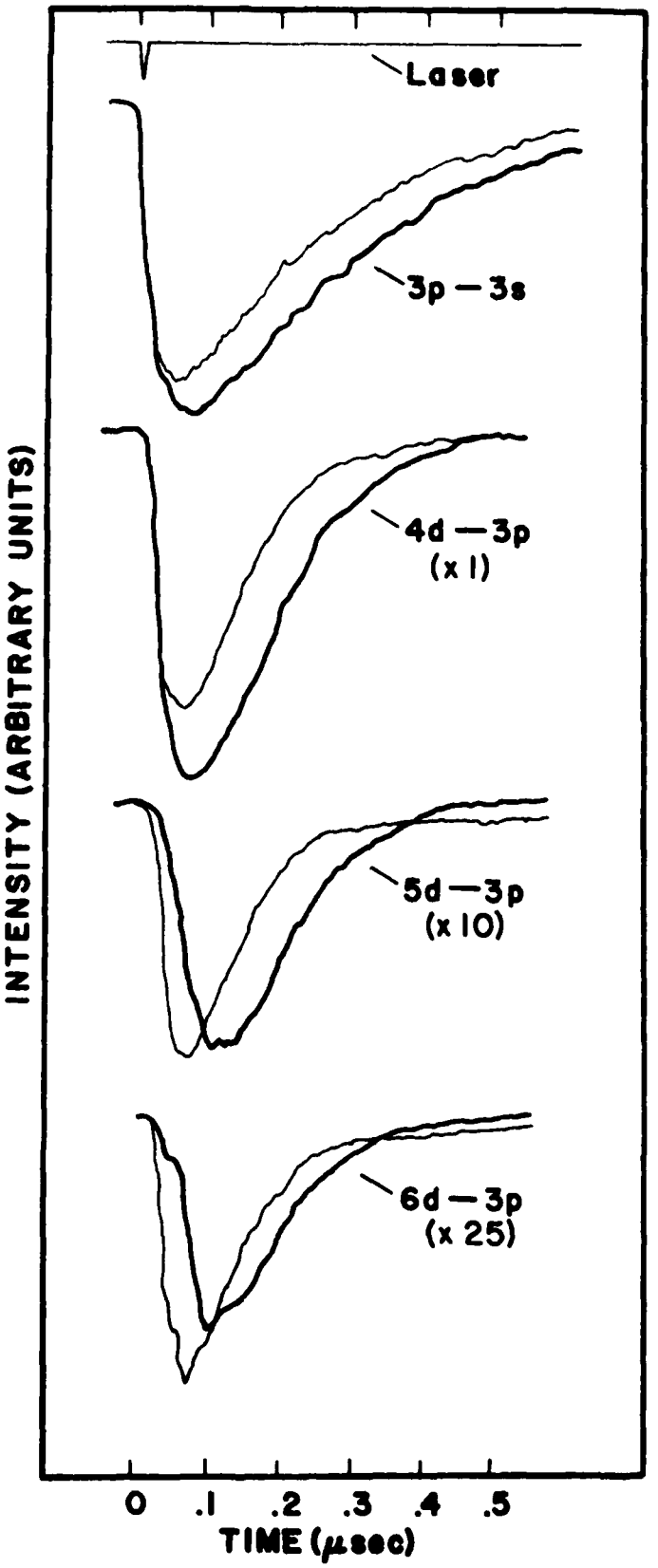
Laser
3p — 3s
4d — 3p
(x 1)
5d — 3p
(x 10)
6d — 3p
(x 25)
INTENSITY (ARBITRARY UNITS)
0
.1
.2
.3
.4
.5
TIME (μsec)

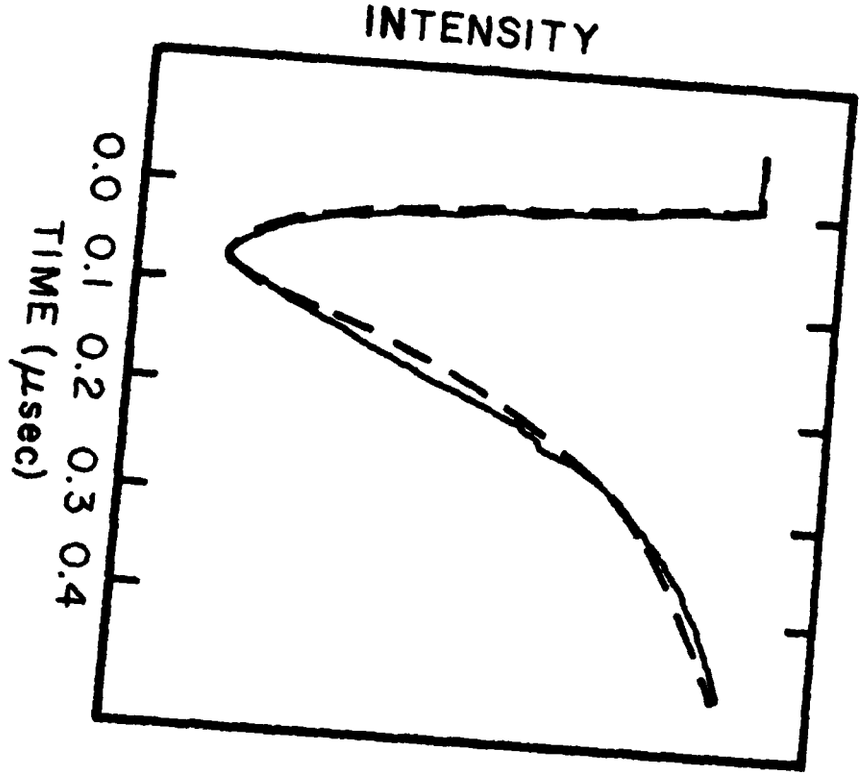
INTENSITY
0.0 0.1 0.2 0.3 0.4
TIME (μsec)

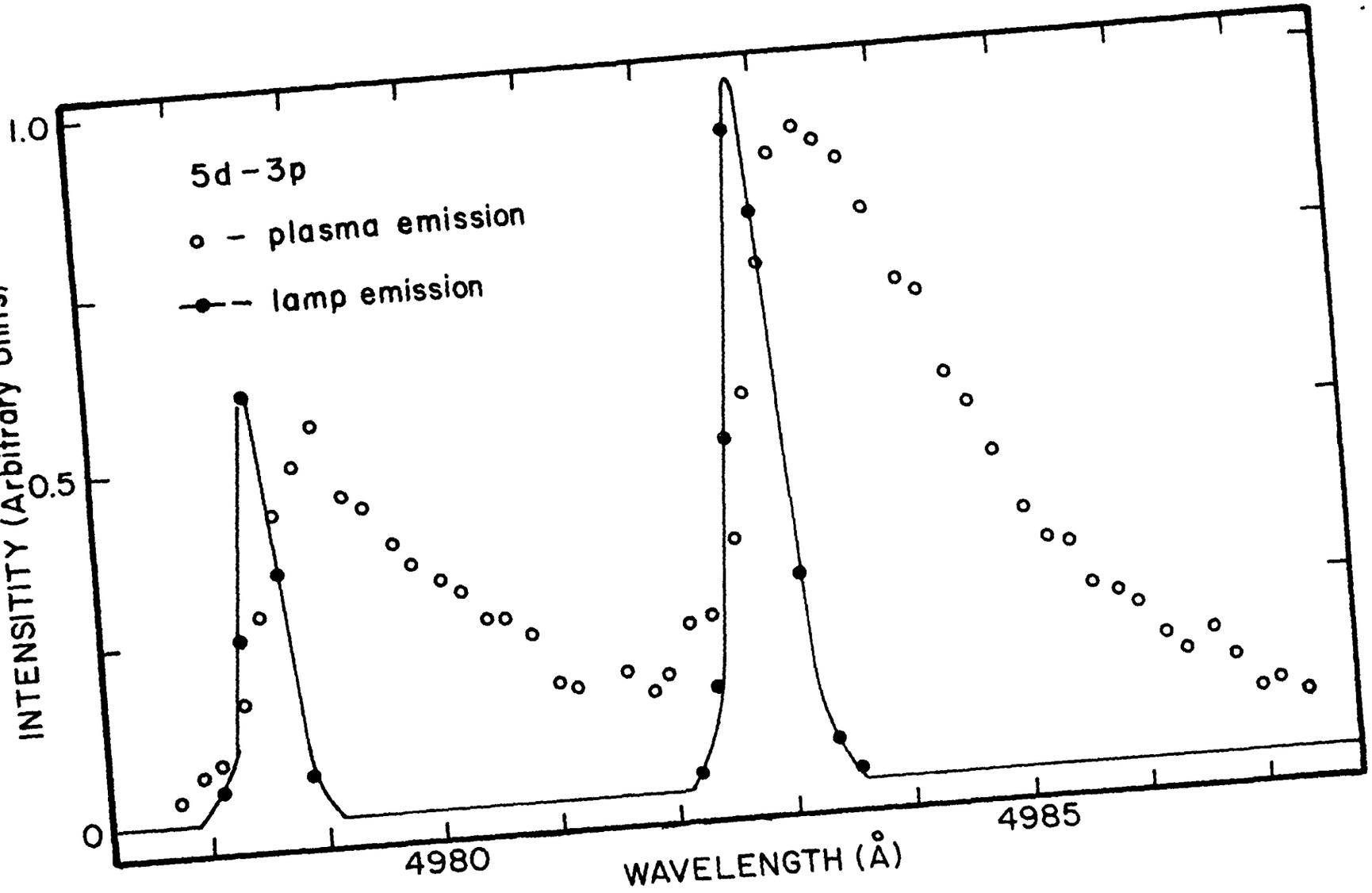
5d – 3p
o – plasma emission
—●— lamp emission
INTENSITY (Arbitrary Units)
1.0
0.5
0
4980
4985
WAVELENGTH (Å)

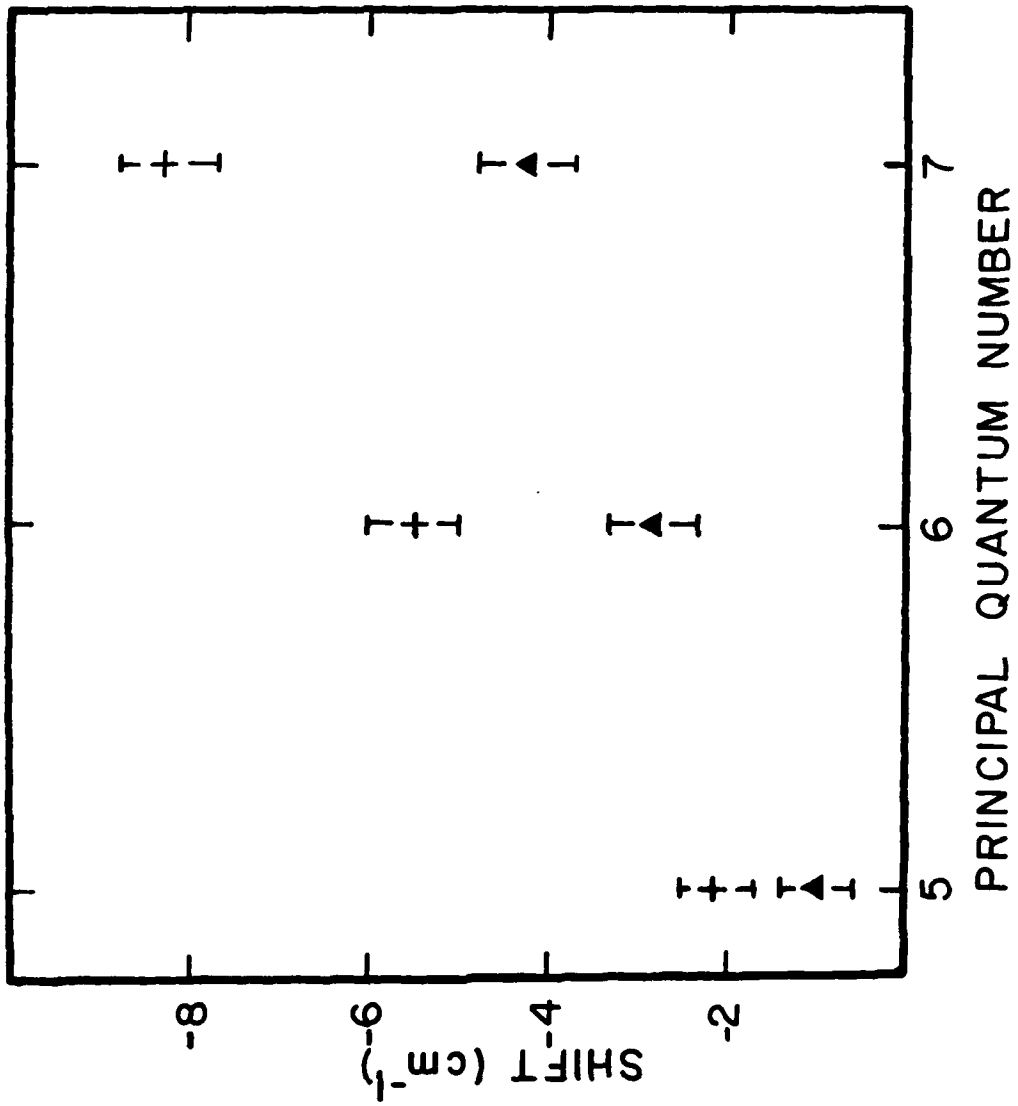
SHIFT (cm⁻¹)
-8
-6
-4
-2
5
6
7
PRINCIPAL QUANTUM NUMBER

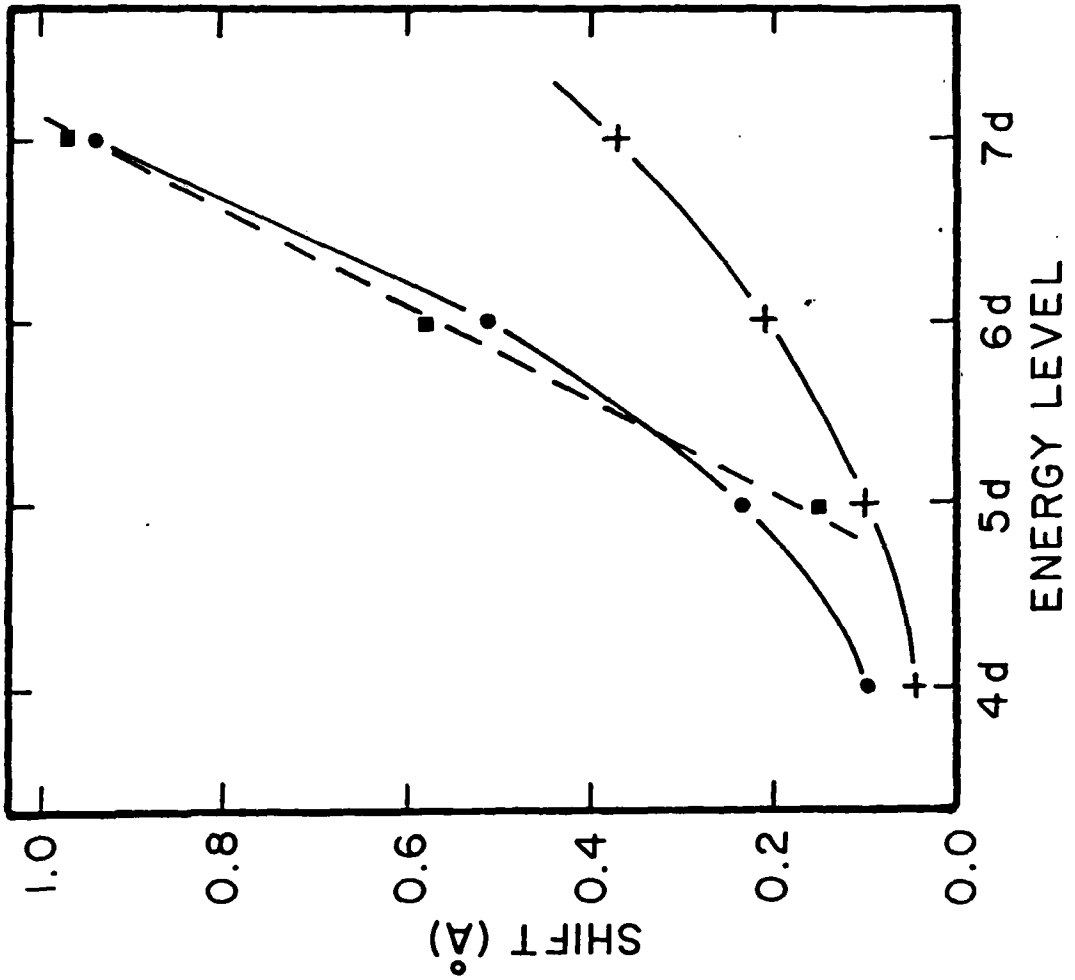
SHIFT (Å)
1.0
0.8
0.6
0.4
0.2
0.0
4d
5d
6d
7d
ENERGY LEVEL

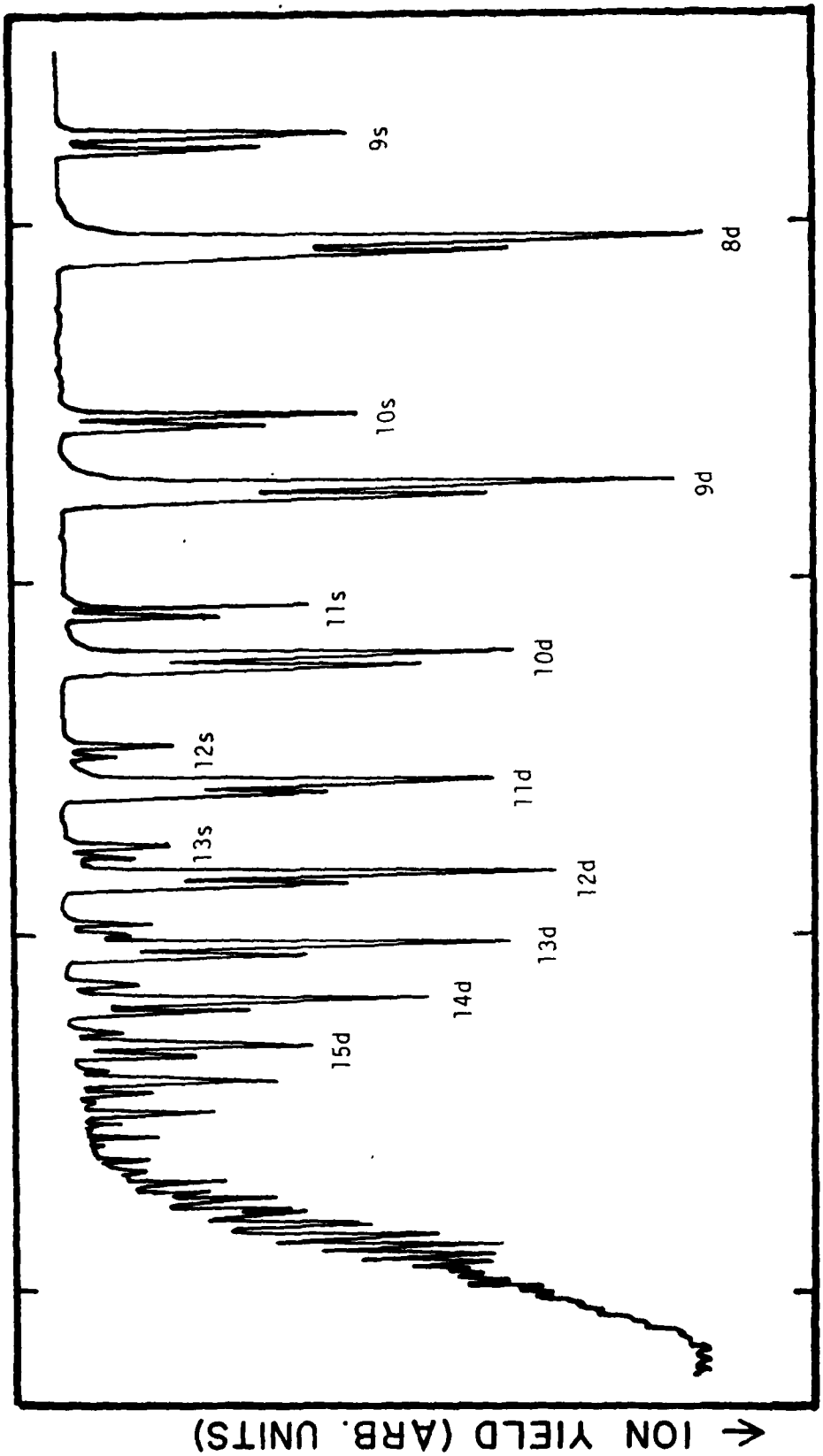
ION YIELD (ARB. UNITS)
410
420
430
440
WAVELENGTH (nm)
9s
8d
10s
9d
11s
10d
12s
11d
13s
12d
13d
14d
15d

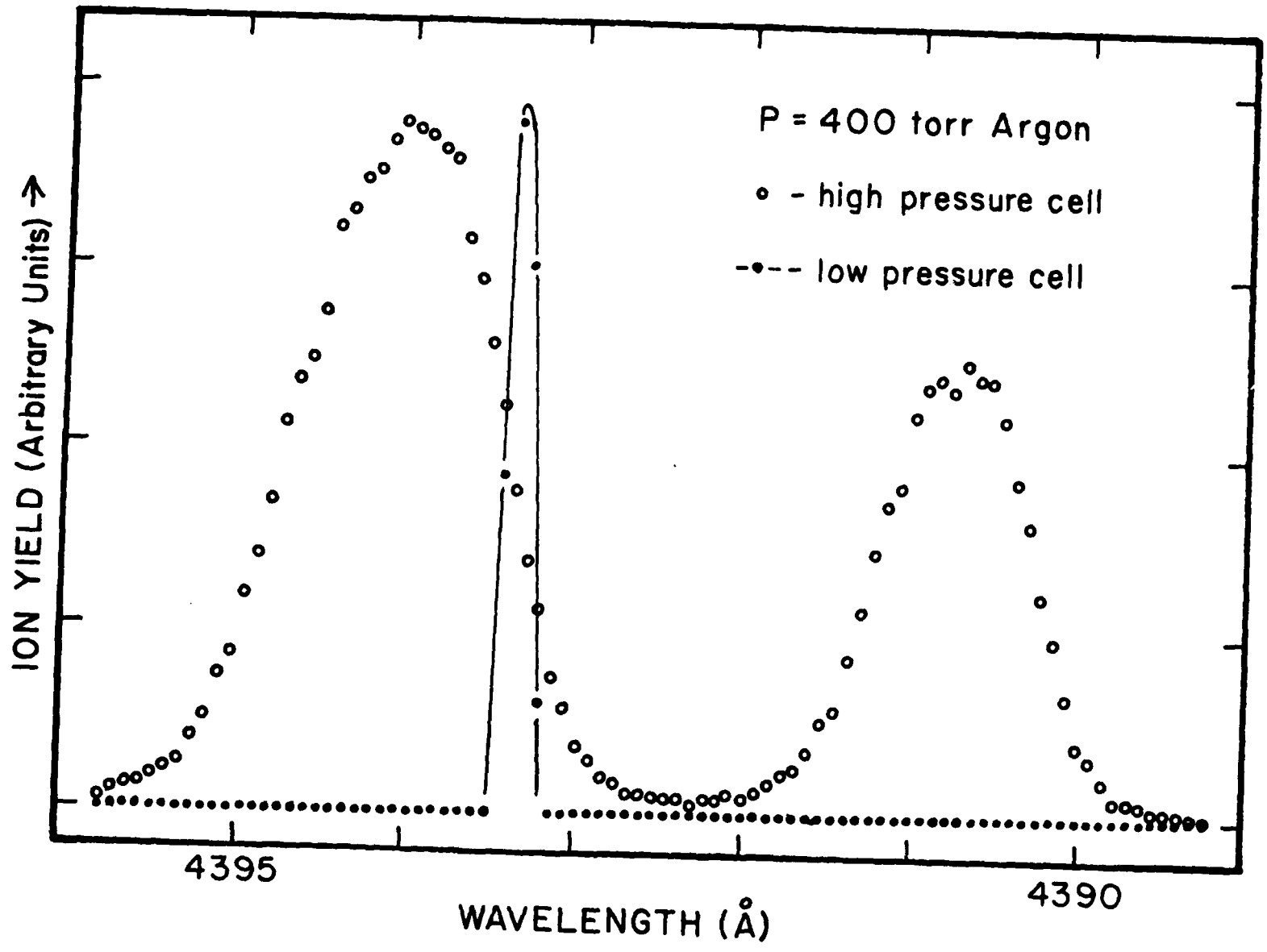
P = 400 torr Argon
o - high pressure cell
--•-- low pressure cell
ION YIELD (Arbitrary Units) →
4395
4390
WAVELENGTH (Å)

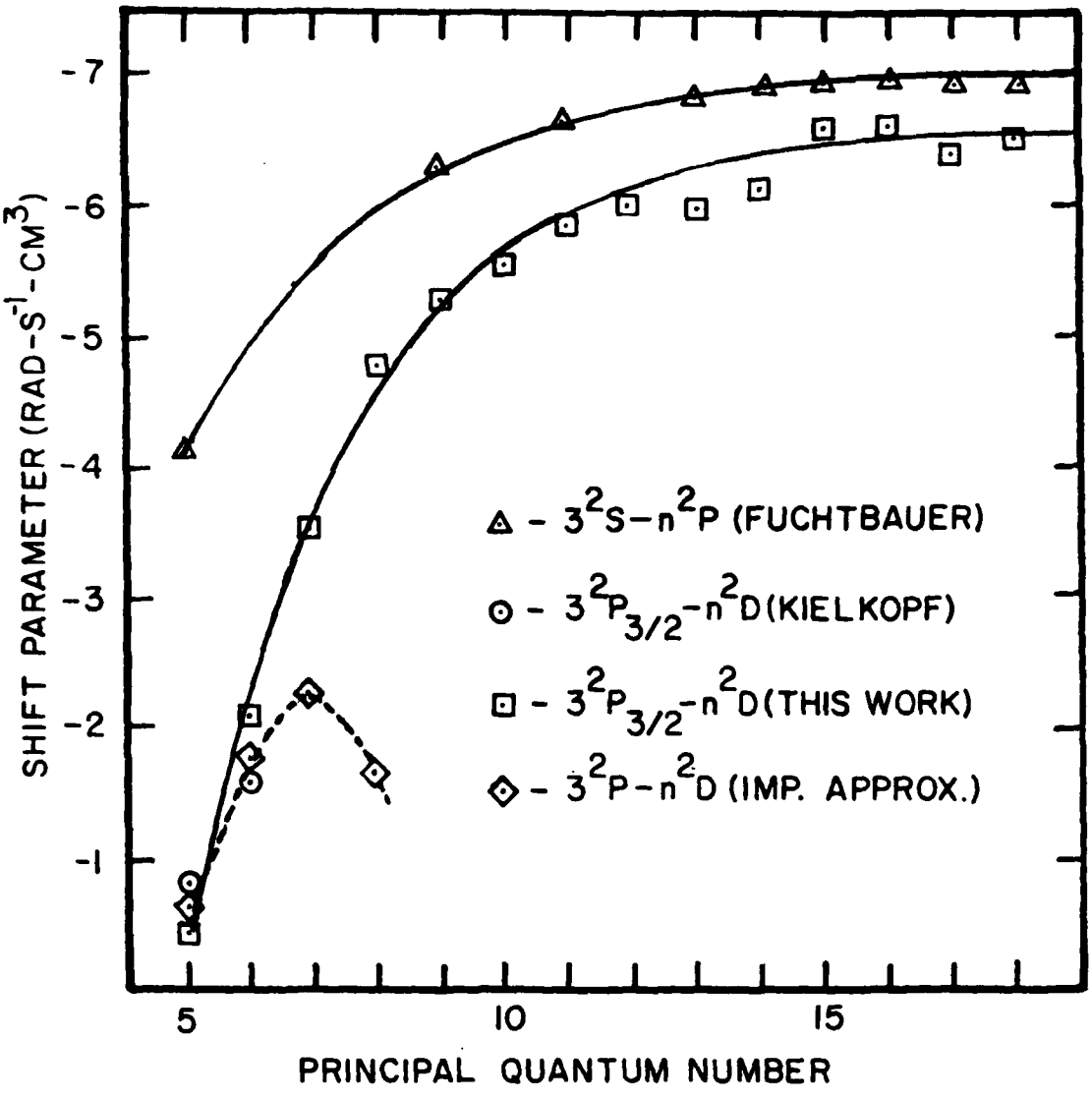
SHIFT PARAMETER (RAD-S^{-1}-CM^3)
-7
-6
-5
-4
-3
-2
-1
5
10
15
PRINCIPAL QUANTUM NUMBER
△ - 3^2S-n^2P (FUCHTBAUER)
⊙ - $3^2P_{3/2}-n^2D$(KIELKOPF)
⊡ - $3^2P_{3/2}-n^2D$(THIS WORK)
◇ - 3^2P-n^2D (IMP. APPROX.)

PUBLICATIONS AND PRESENTATIONS SINCE DECEMBER 1980

Publications

1. "Laser Isotope Dating" (with R. H. McFarland and Javed Husain) in "Nuclear Methods in Environmental and Energy Research", pp. 275-279, ed. by J. R. Vogt, National Technical Information Service, Springfield, VA, Oct. 1981.

2. "Excitation Transfer Collisions and Electron Seeding Processes in a Resonantly Excited Sodium Vapor" (with D. J. Krebs), J. Chem. Phys. 75, 3340 (1981).

3. "A Computer-Controlled, Narrow-Band, Nitrogen-Pumped, Scanning Dye Laser" (with D. J. Krebs), submitted for publication.

4. "Electron Density Measurements in a Laser-Induced Sodium Plasma" (with D. J. Krebs), submitted for publication.

Presentations - contributed

1. "Absorption Profiles for Transitions to Na Rydberg Levels Perturbed by High Concentrations of Argon" (with D. J. Krebs), Bull. Am. Phys. Soc. 26, 727 (1981

2. "Computer Graphics", Kilobaud Microcomputing, May 1981.

3. "Collisional Lineshifts of the 3P-nD Rydberg Transitions of Na by Rare-Gas Atoms and Electrons" (with D. J. Krebs), XIIth International Conference on the Physics of Electronic and Atomic Collisions: Proceedings, Gatlinburg, TN, July, 1981.

4. "Collisional Processes in a Dense Na Vapor following Resonant Excitation by Fast Laser Pulses" (with D. J. Krebs), 34th Annual Gaseous Electronics Conference, Boston, MA, Oct., 1981.

Invited Colloquia

1. University of Missouri-St. Louis, Physics Department, Feb. 1981.

2. University of Arkansas, Physics Department, July 1981.

3. Muhlenberg College, Physics Department, Octo. 1981.

Conferences Attended

1. DEAP, Los Angeles, Dec. 1980.

2. American Physical Society Meeting, NYC, Jan. 1981.

3. Gordon Conference, Atomic Physics, July 1981.

4. XIIth ICPEAC, Gatlinburg, TN, July 1981.

5. 34th GEC, Boston, MA, Oct. 1981.

OTHER FEDERAL SUPPORT

Professor Schearer is the principal investigator on a contract from the Air Force Research Laboratory, WPAFB to investigate dissociative excitation processes involving mercury-halogen systems. Funding for the first year, 1 Aug. 1981 - 31 July 1982, is $25,000.

No other federal funds are available to this investigator.

UNEXPENDED FUNDS

At the expiration of the current contract period, 3/31/82, we anticipate that there will be no unexpended funds remaining.


FILMED
8